LAWRENCE
LIVERMORE
NATIONAL
LABORATORY

LLNL-JRNL-617652

Nanoscale Anisotropic Nd-Fe-B Particles with High Coercivity Prepared by Attrition Milling

C. Wehrenberg, M. Daniil, M. Willard, B. Zande, N. Thadhani

February 11, 2013

Applied Physics Letters

Disclaimer

Nanoscale Anisotropic Nd-Fe-B Particles with High Coercivity Prepared by Attrition Milling

C. Wehrenberg,[1] M. Daniil,[2] M. Willard,[2] B. Zande,[3] S. Sankar,[3] and N. Thadhani[4]
[1)] *Lawrence Livermore National Laboratory, Livermore, CA, 94550*
[2)] *Naval Research Laboratory, Washington DC 20375*
[3)] *Advanced Materials Corporation, Pittsburgh, PA 15220*
[4)] *Georgia Institute of Technology, Atlanta, GA 30332*

Nanoscale Nd-Fe-B particles were fabricated with room temperature coercivity of 4.9 kOe by attrition milling (stirred media milling). In contrast to high-energy milling (SPEX milling), x-ray diffraction (XRD) scans indicate the attrition milled material remains primarily in the crystalline state throughout the milling process. The attrition milling process can yield anisotropic particles, as shown by the creation of strong texture in the XRD patterns by the application of a pulsed magnetic field. For longer milling times, size distributions can be achieved in which >80% of the particles are less than 500 nm in diameter, and a decanting process can be used to obtain particles in the 50-200 nm range. The higher room-temperature coercivity as compared to other magnetic nanoparticles is attributed to the larger size of the particles and the limited plastic deformation created during attrition milling.

I. INTRODUCTION

Interest in fabricating nanoscale magnetic particles has been dramatically increasing in recent years due to their potential for use in exchange-coupled hard/soft nanocomposite permanent magnets. While magnetic models of exchange-coupled nanocomposite magnets have predicted energy products in excess of 1 MJ/cm^3[1], attempts to fabricate such magnets have faced several challenges, such as consolidation to full density without grain growth or development of texture. Nanocomposite magnetic powders formed from ball-milling[2] or melt-spinning[3] have been successfully consolidated without grain growth through shock compaction[4,5] or careful control of warm pressing conditions.[6] However, efforts to introduce texture into nanocomposite materials through the die-upsetting process have been only partially successful.[7,8]

Using an alternative approach, isotropic magnets have been fabricated by mixing FePt and Fe_3O_4 nanoparticles and consolidating the mixture by warm compaction.[9] This technique could potentially lead to highly textured microstructures by applying external magnetic fields, but practical applications have been limited by the low coercivity of the materials. Recently, nanometer sized particles have been synthesized in material systems which typically yield high coercivity, such as $Nd_2Fe_{14}B$, through surfactant assisted high energy ball milling (SA-HEBM); however, these nanoparticles have also exhibited low coercivity, ranging from 0.1 to 1.8 kOe at room temperature.[10–12]

This paper will study the attrition milling process for fabrication of high coercivity submicron and nanoscale $Nd_2Fe_{14}B$ particles. While the technique of attrition milling (stirred media milling) has been known to produce particles sizes in the 100 nm range in some materials,[13] application of the technique to Nd-Fe-B has been previously limited to particle sizes in the tens of microns range.[14] We demonstrate that submicron and nanometer sized particles can be produced with this method, and that these particles exhibit anisotropy and significantly higher coercivity at room temperature than reports for alternative fabrication methods. The relationship between the coercivity and the amount of plastic deformation produced during milling will also be studied.

II. EXPERIMENTAL PROCEDURE

Nd-Fe-B powder produced by the hydrogenation-decomposition-desorption-recombination (HDDR) method with a nominal composition of $(Nd,Dy)_{15}(Fe,Co)_{79}B_6$ was provided by Magnequench, Inc. Energy dispersive spectroscopy (EDS) performed on the powder showed that the ratio of iron to cobalt content was approximately 3:1, while the amount of dysprosium was too small to be reliably measured by this technique.

For comparison purposes, milling was performed using either the attrition milling or the high energy ball milling (HEBM) method. Attrition milling was performed using a Union Process Model 01 attritor mill. A polypropylene jar was used as the milling vial with 1/8" steel balls in a 1:1 ball to powder mass ratio in toluene slurry. The stirring speed was approximately 4 Hz. Toluene was removed from milled samples by placing them in a vacuum for 24 hours. High energy ball milling was performed without slurry using 1/4" steel balls in a 1:1 ratio on a SPEX 8000 mill. The powder and milling media were handled and sealed inside a glove box with an argon environment.Stirred media milling was performed for milling times up to 400 hours while HEBM was performed for up to 12 hours.

The structure and morphology of the milled particles were studied using a LEO 1550 scanning electron microscope (SEM) and a Phillips MRD x-ray diffractometer. XRD was performed using copper K_α radiation. Jade XRD analysis software was used to remove back-

ground and $K_{\alpha 2}$ radiation and to fit diffraction peaks to a pseudo-Voigt (combined Gaussian-Lorentzian) curve. Magnetic measurements were performed on a Quantum Design Magnetic Property Measurement System (SQUID magnetometer) with maximum field of 50 kOe. Powder samples were mounted in paraffin wax at ∼50°C to prevent rotation during SQUID measurements. The mass of the SQUID samples was measured using a Sartorius CP2P microbalance prior to encasing in paraffin. The saturation magnetization was found using the law of approach.[15]

Alignment of the milled particles was performed at Advanced Materials Corporation. The powders were pressed by hand into a 0.5" polyurethane die and sealed inside a rubber bag. Three 10 T magnetic field pulses of ∼50 ms duration were applied to each sample. Samples were then pressed isostatically at 30-34 ksi to allow the samples to be handled without further altering the alignment.

III. RESULTS

Figure 1 SEM images were recorded for samples taken at various times of the milling process to monitor the evolution of the particle morphology. Figure 1 compares SEM images of the Nd-Fe-B starting powder with a sample after 185 hours of attrition milling. The original particles, Figure 1 (a), have a wide range of sizes, from a few microns up to a few hundred microns. For the attrition milled powder in part (b), the particle size has decreased significantly, with nearly all particles being submicron. The grain morphology of the original particles, shown in the high magnification inset in part (a), is spheroidal with a typical diameter of 200-400 nm and is roughly similar to the particle morphology of the milled powder shown in part (b).

The number percentage for four size groups, >1000 nm, 1000-500 nm, 500-250 nm, and <250 nm, was measured from multiple SEM images of attrition milled particles. Figure 2 shows the subsequent size distribution for several milling times. The size distribution moves towards smaller particle sizes with increasing milling time, up to 185 hours, with no further size reduction for 400 hours milling time. At this point, most particles (∼85%) are smaller than 500 nm. The size distribution of the starting powder is not shown, as it is almost entirely >1000 nm.

Figure 3 shows the room temperature magnetic hysteresis curve for the starting powder and attrition milled Nd-Fe-B particles after 185 hours of attrition milling. The magnetic saturation in the milled powder (141 emu/g) has decreased slightly relative to the starting powder (145 emu/g). This is most likely due to surface oxidation which occurs during handling. While attrition milling yields a lower coercivity than the starting powder, the milled powder maintains a room temperature coercivity of 4.9 kOe. This coercivity value is significantly higher than the coercivity of nanoparticles formed by surfactant-assisted ball milling, which can range from 0.1 kOe to 1.8 kOe, depending on the size of the particles and the processing route.[11,16]

Figure 4 shows XRD traces for attrition milled powder with run times of 40 and 185 hours, along with the pattern for the starting powder. No oxidation lines were

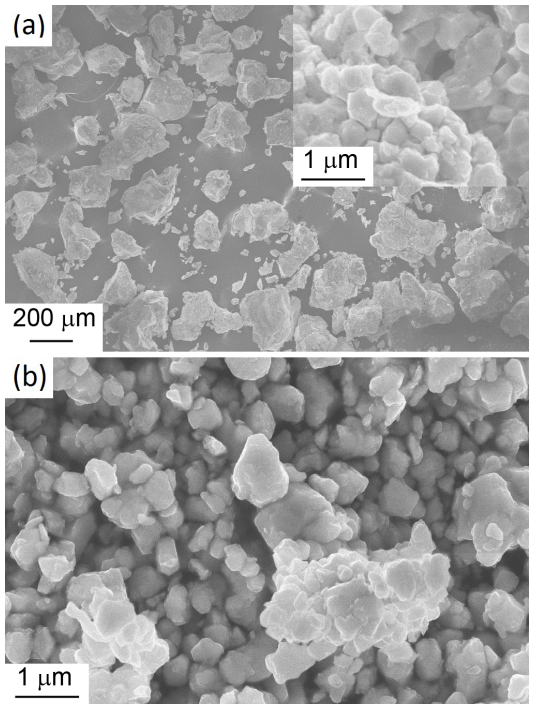

FIG. 1. SEM images of (a) HDDR Nd-Fe-B starting powder with high magnification inset showing grain morphology and (b) powder after 185 hours of attrition milling.

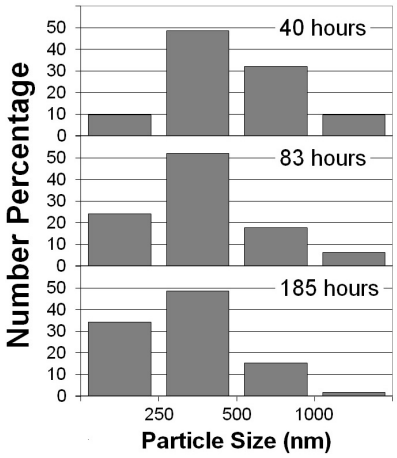

FIG. 2. Size distribution of attrition milled Nd-Fe-B powder. Number percentages are shown for size groups of <250 nm, 250-500 nm, 500-1000 nm, and >1000 nm. Nearly all particles in the as-received powder are larger than 1000 nm. Milling for 400 hours does not produce a size distribution significantly different that the 185 hour samples.

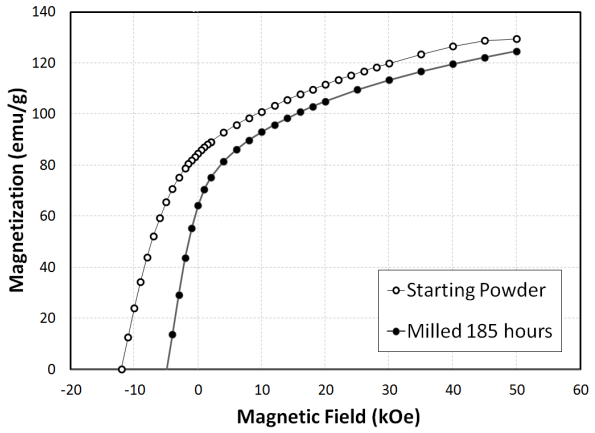

FIG. 3. Magnetic hysteresis curve for starting powder and particles milled for 185 hours.

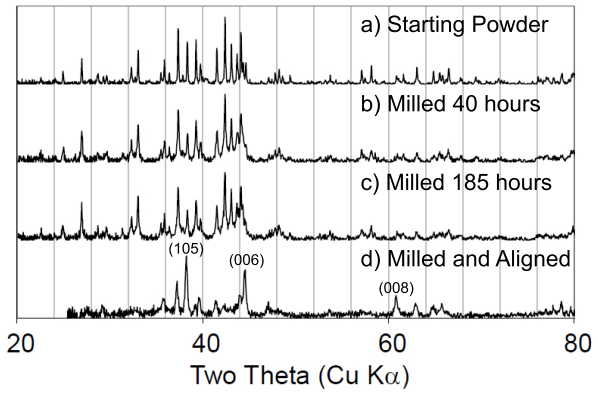

FIG. 4. XRD traces of (a) HDDR Nd-Fe-B starting powder, samples milled for (b) 40 and (c) 185 hours, and (d) milled powder (185 hrs) after alignment by pulsed magnetic field.

observed in the milled powder, which is consistent with a small decrease in saturation magnetization. The milled powders show only a slight increase in diffraction peak widths; however, Williamson-Hall analysis did not yield identifiable trend lines. The XRD trace in part (d) shows the 185 hour milled powder after alignment in a pulsed magnetic field. The (00c) family of peaks and the (105) peak, which is oriented only 11.3° from the (00c) planes, have all increased in relative intensity, indicating that the particles are primarily anisotropic with an easy magnetization axis oriented along the c-axis.

HEBM studies were performed to serve as a comparison to attrition milling. Figure 5 displays XRD traces for the as-received powder and samples that have undergone HEBM for 2 hours and 8 hours. As milling time increases, the diffraction peak widths show a much larger increase than the peaks in the attrition milled scan. At 8 hours of milling time, the diffraction peaks have broadened to such an extent that the pattern resembles that of an amorphous material. Similar results, in which HEBM of Nd-Fe-B produces α-Fe and amorphous Nd-Fe-B, have been previously reported in the literature.[17] In addition

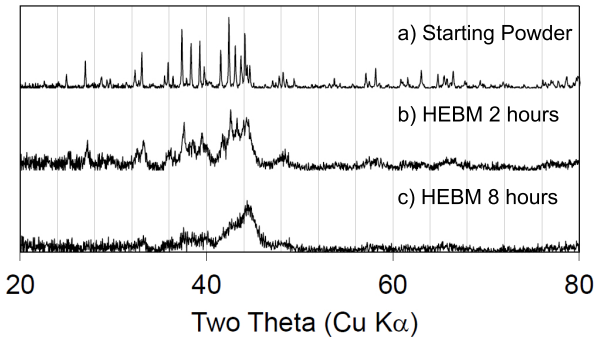

FIG. 5. XRD traces of high-energy ball milled HDDR Nd-Fe-B powder (a) as-received (b) milled for 2 hours and (c) milled for 8 hours.

to the wide differences in time scales, the XRD results show that the two forms of ball milling produce markedly different effects in the material, with HEBM producing significantly more peak broadening than attrition milling and eventually a transition to the amorphous state.

IV. DISCUSSION

The relatively high coercivity of the attrition milled particles as compared to reports of surfactant-assisted HEBM is most likely due to the larger size of the particles and to the smaller amount of defects produced during attrition. SA-HEBM can produce particles as small as 2 nm[12], and one would expect significant surface effects at this size. In addition, the XRD results suggest only a small amount of defects due to plastic deformation are present in the attrition milled powder. While Williamson-Hall plots did have identifiable trend lines, the typical diffraction peak width of the starting powder (0.07-0.10° at half maximum) is similar to the LaB_6 diffraction standard (0.07-0.08°), indicating limited broadening from retained microstrain or small crystallite size. Diffraction peak widths increased only slightly for both 40 and 185 hour run times to 0.1-0.4° and 0.1-0.5° respectively. In contrast, HEBM produces extensive peak broadening, leading to a transition to the amorphous state.

The contrasting effects produced by the two forms of ball milling are most likely the result of the different mechanical loading conditions experienced during the two processes. The free flight and resulting collisions that occur in HEBM produces higher stresses and strain rates than those created during the grinding-like action of attrition milling. While both milling processes occur through a combination of deformation and fracture, the lower stress and strain rate of the attrition milling process may lend itself to producing more particle fracture than HEBM. This is corroborated by the ability of attrition milled particles to be aligned in a magnetic field, as seen in part (d) of Figure 4, since a milling pro-

cess which proceeds mainly by fracture is more likely to produce anisotropic particles than one which produces large amounts of plastic deformation. Attempts to align HEBM material using similar pulsed magnetic fields results in no significant changes in the XRD patterns, indicating the particles are isotropic. In addition, the observation, as seen in Figure 1, that the attrition milled particles have a similar morphology to the grains of the starting material, suggests that fracture may occur primarily along grain boundaries during attrition milling.

While the size of the particles studied in the work is significantly larger than the size that has been recommended for ultra high energy products (2-3 nm thick layers)[1], they are still sufficiently small to allow a composite to be created with a significant amount of soft phase. Micromagnetic studies have shown that the energy product and remanence enhancement in exchange coupled nanocomposite magnets are very sensitive to the size of the soft phase[18]; however, such studies often assume the hard phase to be many times larger than the soft phase.[19] Thus, the size of the hard phase is not limited by exchange coupling restrictions, but by geometry and the necessity of avoiding clusters of the soft phase grains. If the grain size of the hard phase is very large (>1 μm), then the soft phase must either be too large (or clustered) to make a suitable composite or comprise a very small fraction of the total magnet.

Using the size distribution shown in Figure 2, it is possible to estimate the maximum amount of soft phase that could be added to the attrition milled material to form a suitable composite. If one assumes that a 20 nm coating of soft phase material is added to a particle equal in diameter to the midpoint of each size range, then ∼10-15% soft phase could be added to the 185 hour milled powder. The soft phase percentage can obviously be improved by using even smaller hard phase particles. Nd-Fe-B particles in the 50-200 nm range can be selected from the attrition milled powder by a simple decanting procedure. An SEM image of the selected nanoparticles is shown in Figure 6. While selection of smaller size nanoparticles reduces the total yield of usable nanoparticles, one advantage of the attrition milling technique is the formation of a large volume of milled material, such as the 0.5-1.0 kg batches produced in this work, which illustrates that the attrition milling is a scalable process.

V. CONCLUSIONS

Submicron and nanosized particles of Nd-Fe-B were fabricated through an attrition milling process. Extending milling times up to 185-400 hours yields a particle size distribution with the majority (∼85%) of particles being smaller than 500 nm. The attrition milled powder has a room temperature coercivity (4.9 kOe) significantly higher than nanoparticles fabricated by SA-HEBM. The high coercivity is most likely due to the larger size of the particles and the limited plastic deformation created during attrition milling, as shown by peak broadening in XRD patterns.While the attrition milled particle size is significantly larger than SA-HEBM particles, it is theoretically small enough to allow the formation of hard/soft composites with a significant fraction of soft phase without geometrically requiring clusters of soft phase particles. In addition, particles in the 50-200 nm size range can be selected from the milled powder by a simple decanting procedure. These results show that attrition milling is a promising technique for fabrication of Nd-Fe-B nanoparticles for use in nanocomposite permanent magnets.

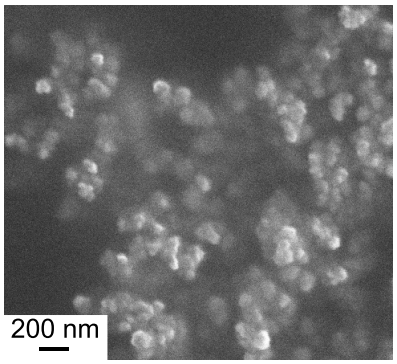

FIG. 6. SEM image of Nd-Fe-B nanoparticles separated from the attrition milled powder by a decanting process.

ACKNOWLEDGMENTS

The authors would like to thank Peter Marshall and Will Daloz for their help with attrition milling and Jennifer Breidenich for her advice on separation of nanoparticles. Funding for this work was provided by DARPA/ARO Grant No. W911NF-08-1-0249. This work performed under the auspices of the U.S. Department of Energy by Lawrence Livermore National Laboratory under Contract DE-AC52-07NA27344.

[1] R. Skomski and J. M. D. Coey, Phys. Rev. B **48**, 15812 (1993).
[2] K. Raviprasad, M. Funakoshi, and M. Umemoto, Journal of Applied Physics **83**, 921 (1998).
[3] Z. Chen, Y. Zhang, Y. Ding, G. Hadjipanayis, Q. Chen, and B. Ma, Journal of Magnetism and Magnetic Materials **195**, 420 (1999).
[4] Z. Q. Jin, K. H. Chen, J. Li, H. Zeng, S. F. Cheng, J. P. Liu, Z. L. Wang, and N. N. Thadhani, Acta Materialia **52**, 2147 (2004).
[5] Z. Q. Jin, N. N. Thadhani, M. McGill, J. Li, Y. Ding, Z. L. Wang, H. Zeng, M. Chen, S. Cheng, and J. P. Liu, Journal of Applied Physics **96**, 3452 (2004).
[6] C. Rong, Y. Zhang, N. Poudyal, X. Xiong, M. J. Kramer, and J. P. Liu, Applied Physics Letters **96**, 102513 (2010).
[7] D. Lee, J. S. Hilton, C. H. Chen, M. Q. Huang, Y. Zhang, G. C. Hadjipanayis, and S. Liu, IEEE Transactions on Magnetics **40**, 2904 (2004).
[8] A. M. Gabay, Y. Zhang, and G. C. Hadjipanayis, Applied Physics Letters **85**, 446 (2004).
[9] C. Rong, V. Nandwana, N. Poudyal, J. P. Liu, M. E. Kozlov, R. H. Baughman, Y. Ding, and Z. L. Wang, J. Appl. Phys. **102**, 023908 (2007).

[10]V. M. Chakka, B. Altuncevahir, Z. Q. Jin, Y. Li, and L. J. P., Journal of Applied Physics **99**, 08E912 (2006).
[11]M. Yue, Y. P. Wang, N. Poudyal, C. B. Rong, and J. P. Liu, Journal of Applied Physics **105**, 07A708 (2009).
[12]N. G. Akdogan, W. Li, and G. C. Hadjipanayis, Journal of Applied Physics **109**, 07A759 (2011).
[13]M. Rahaman, "Ceramic Processing," (CRC, Boca Raton, 2006) Chap. Synthesis of Powders.
[14]P. J. McGuiness, R. Harris, E. Rozendaal, J. Ormerod, and M. Ward, Journal of Material Science **21**, 4107 (1986).
[15]B. D. Cullity and C. D. Graham, "Introduction to Magnetic Materials," (Wiley, Hoboken, 2008) Chap. 9: Domains and the Magnetization Process.
[16]N. G. Akdogan, G. C. Hadjipanayis, and D. J. Sellmyer, Nanotechnology **21**, 295705 (2010).
[17]P. McCormick, W. Miao, P. Smith, J. Ding, and R. Street, Journal of Applied Physics **83**, 6256 (1998).
[18]R. Fischer, T. Schrefl, H. Kronmüller, and J. Fidler, Journal of Magnetism and Magnetic Materials **150**, 329 (1995).
[19]T. Leineweber and H. Kronmüller, Physica Status Solidi (b) **201**, 291 (1997).